Collective nature of low-lying excitations in ^{70,72,74}Zn from lifetime measurements with the plunger technique and the AGATA demonstrator

C. Louchart,[1] A. Obertelli,[1] A. Görgen,[1,2] W. Korten,[1] D. Bazzacco,[3] E. Clément,[3] L. Corradi,[4] G. de Angelis,[4] J.-P. Delaroche,[5] A. Dewald,[6] F. Didierjean,[7] M. Doncel,[8] G. Duchêne,[7] M.N. Erduran,[9] E. Farnea,[10] C. Finck,[7] E. Fioretto,[4] C. Fransen,[6] A. Gadea,[11] M. Girod,[5] A. Gottardo,[4] M. Hackstein,[6] T. Huyuk,[11] A. Kusoglu,[12] S. M. Lenzi,[10] J. Ljungvall,[13,1] S. Lunardi,[10] D. Mengoni,[14,4] R. Menegazzo,[10] C. Michelagnoli,[10] O. Möller,[15] G. Montagnoli,[10] D. Montanari,[10] D.R. Napoli,[4] R. Orlandi,[16] G. Pollarolo,[17] A. Prieto,[8] B. Quintana,[8] F. Recchia,[10] W. Rother,[6] E. Sahin,[10] M.-D. Salsac,[1] F. Scarlassara,[10] S. Siem,[18] P.P. Singh,[4] A.M. Stefanini,[4] O. Stézowski,[19] B. Sulignano,[1] S. Szilner,[20] C. Ur,[21] J.J. Valiente-Dobón,[4] and M. Zielinska[1]

[1] *CEA, Centre de Saclay, IRFU/Service de Physique Nucléaire, F-91191 Gif-sur-Yvette, France*
[2] *Present address:University of Oslo, Department of Physics, N-0316 Oslo, Norway*
[3] *GANIL, CEA/DSM-CNRS/IN2P3, F-14076 Caen Cedex 05, France*
[4] *INFN, Laboratori Nazionali di Legnaro, Legnaro (Padova), Italy*
[5] *CEA, DAM, DIF, F-91297 Arpajon, France*
[6] *IKP, Universitätt zu Köln, Germany*
[7] *IPHC, IN2P3/CNRS et Université Louis Pasteur, Strasbourg, France*
[8] *LRI, Salamanca University, Spain*
[9] *Istanbul Sabahattinn Zaim University, Istanbul, Turkey*
[10] *INFN Sezione di Padova and Dipartimento di Fisica, Università di Padova, I-35131 Padova, Italy*
[11] *IFIC Valencia, Spain*
[12] *Department of Physics,Istanbul University, Istanbul, Turkey*
[13] *Centre de Spectrométrie Nucléaire et de spectrométrie de Masse - CSNSM, CNRS/IN2P3 and Université Paris-Sud, F-91405 Orsay campus, France*
[14] *School of Engineering, University of the West of Scotland, Paisley, UK*
[15] *Institut für Kernphysik, Darmstadt, Germany*
[16] *University of the West of Scotland, Scotland*
[17] *Dipartimento di Fisica Teorica, University of Torino and INFN, Sezione di Torino, Italy*
[18] *Department of Physics, University of Oslo, Norway*
[19] *Université de Lyon, Université Lyon 1, CNRS-IN2P3, Institut de Physique Nucléaire de Lyon, F-69622 Villeurbanne, France*
[20] *Ruder Boskovic Institute, Zagreb, Croatia*
[21] *Dipartimento di Fisica, Università di Padova and INFN, Italy*

Background: Neutron-rich nuclei with protons in the fp shell show an onset of collectivity around N=40. Spectroscopic information is required to understand the underlying mechanism and to determine the relevant terms of the nucleon-nucleon interaction that are responsible for the evolution of the shell structure in this mass region. **Methods:** We report on the lifetime measurement of the first 2^+ and 4^+ states in ^{70,72,74}Zn and the first 6^+ state in ^{72}Zn using the Recoil Distance Doppler Shift method. The experiment was carried out at the INFN Laboratory of Legnaro with the AGATA demonstrator, first phase of the Advanced Gamma Tracking Array of highly segmented, high-purity germanium detectors coupled to the PRISMA magnetic spectrometer. The excited states of the nuclei of interest were populated by deep inelastic scattering from a ^{76}Ge beam impinging on a ^{238}U target. **Results:** The maximum of collectivity along the chain of Zn isotopes is observed at N=42. An unexpectedly long lifetime of $20^{+1.8}_{-5.2}$ ps was measured for the 4^+ state in ^{74}Zn. **Conclusions:** Our results lead to small values of $B(E2;4_1^+ \rightarrow 2_1^+)/B(E2;2_1^+ \rightarrow 0_1^+)$ for ^{72,74}Zn, suggesting a significant non-collective contribution to these excitations. These experimental results are not reproduced by state-of-the-art microscopic models and call for lifetime measurements beyond the first 2^+ state in heavy zinc and nickel isotopes.

PACS numbers: 21.10.Ky, 23.20.-g, 27.50.+e, 29.30.Kv, 29.40.Gx

I. INTRODUCTION

The well known magic numbers observed in spherical nuclei, which are at the basis of the nuclear shell model, were explained by Goeppert-Mayer and Jensen by introducing a spin-orbit term to the one-body nuclear potential [1–3]. While moving toward the neutron drip line, the quenching of shell gaps and the emerging of new shell closures have been observed. For instance, it has been shown experimentally that the N = 20 gap vanishes [4, 5], while at the same time a new shell closure appears at N = 16 [6, 7]. Specific terms of the nucleon-nucleon (NN) interaction are proposed to be at the origin of this evolution of the nuclear shell structure. The spin-isospin and tensor terms have been suggested to play a crucial role in the structure in light and medium-mass neutron

rich nuclei [8, 9]. More recently, the three-body force was claimed to impact the magic number picture across the nuclear chart [10, 11].
A very interesting region, presently accessible experimentally and where sudden structural changes occur, is the one around ^{68}Ni. Here, it is possible to trace the evolution of single-particle states with neutron number by performing spectroscopy of odd-mass nuclei. As an example, the $\pi f_{5/2}$ orbital is found to drop sharply with neutron number in neutron-rich Cu isotopes and cross the $\pi p_{3/2}$ orbital to become the ground-state at N=46 in ^{75}Cu [12, 13]. The consequences of such orbital migrations for even-even nuclei can be investigated by measuring $B(E2)$ values.

The lifetime of the first 2^+ state in an even-even nucleus is, in general, inversely proportional to the reduced transition probability, $B(E2; 2_1^+ \rightarrow 0_1^+)$, and gives a first indication of the collectivity of the nucleus. The small $B(E2; 2_1^+ \rightarrow 0_1^+)$ value together with the high excitation energy of the 2_1^+ state in ^{68}Ni, although suggesting at first sight a sub-shell closure, has been shown to be a local feature arising from the parity change of the νf$_{5/2}$-νg$_{9/2}$ orbitals that define the N = 40 gap. Indeed, adding two neutrons to the νg$_{9/2}$ orbital, ^{70}Ni exhibits a large $B(E2)$ [14]. Furthermore, recent $B(E2)$ measurements for ^{64}Fe and ^{66}Fe, with two proton holes in the ^{68}Ni, found a sudden and strong increase of collectivity when approaching N = 40, which cannot be reproduced by considering only the νf$_{5/2}$pg$_{9/2}$ shell-model valence space [15, 16]. Recent Shell Model calculations using a larger valence space (pf shell for protons and $pfg_{9/2}d_{5/2}$ for neutrons with a ^{48}Ca core) [17] indicate an important role of the νd$_{5/2}$ orbital to describe the onset of collectivity below ^{68}Ni. Similar conclusions have been drawn from the spectroscopy of neutron-rich Cr isotopes [18, 19] and are supported by recent mass measurements of heavy manganese isotopes [20]. A slightly increasing occupation of the νd$_{5/2}$ orbital in Fe isotopes with increasing neutron number is also predicted by beyond mean-field calculations [21], but remains small. The importance of the νd$_{5/2}$ orbit in this mass region still needs further investigation outside the Z = 28 Ni core. In this respect, the evolution of collectivity in Zinc isotopes, with two more protons than Ni, should bring valuable information on the filling of the νd$_{5/2}$ orbital with an increasing number of neutrons in the vicinity of N = 40. The systematics of $B(E2)$ values for the $^{74-80}$Zn isotopes, extracted from Coulomb excitation experiments with radioactive ion beams [22], suggests a maximum of collectivity for N = 44. A recent lifetime measurement of the 2_1^+ state in ^{74}Zn [23] found a lower value than previous published results from Coulomb excitation at both intermediate energy [14] and low energy [22]. In the case of Se and Ge isotopes, a maximum of collectivity is found at N = 42.

While the measurement of $B(E2; 2_1^+ \rightarrow 0_1^+)$ values is very useful to investigate the evolution of collectivity along isotopic or isotonic chains, more insight into the collective behavior of a given nucleus can be gained from measuring the lifetimes of higher-lying states. The various ratios of $B(E2)$ values between different states are characteristic for different types of rotational or vibrational excitations. The ratio $B(E2; 4_1^+ \rightarrow 2_1^+)/B(E2; 2_1^+ \rightarrow 0_1^+)$, for example, is expected to take the value $B_{42} = 2.0$ for a harmonic vibration and $B_{42} = 1.43$ for a rigid rotation, respectively. Only in case of non-collective nuclei at or near closed shells does one expect the above ratio to be less than unity. Very few cases of collective nuclei with anomalously low B_{42} ratio have been identified in the literature [24], but some of them turned out to be due to flawed measurements [25, 26].

In this article we report on lifetime measurements of short-lived excited states in ^{70,72,74}Zn using the Recoil-Distance Doppler Shift method with the AGATA Demonstrator [27, 28], the first phase of the European Advanced GAmma Tracking Array based on highly segmented germanium detectors. The experimental setup will be described in section II, details on the data analysis are given in section III whereas section IV gathers a discussion on the obtained results.

II. EXPERIMENTAL SETUP

Neutron-rich Zn isotopes were produced by multi-nucleon transfer induced by a ^{76}Ge beam impinging onto a ^{238}U target. The beam was delivered by the LNL Tandem-ALPI accelerator complex at an energy of 577 MeV. The metallic ^{238}U target of 1.4 mg/cm^2 thickness was evaporated onto a 1.2 mg/cm^2 Ta backing, which was facing the beam at an angle of 45°. The beam energy at the center of the target was approximately 540 MeV. During the experiment the beam intensity was maintained at 11 enA. The projectile-like reaction products were identified at the focal plane of the magnetic spectrometer PRISMA [29] rotated to the grazing angle of 55° with respect to the beam axis. PRISMA is composed of a quadrupole and a dipole magnet. The magnetic rigidity of the spectrometer was set to Bρ = 0.86 Tm. The focal plane comprises a row of 10 Parallel Plate Avalanche Counters (PPAC) [30] and ionization chamber decomposed in 40 sections (10 raws and 4 subsections each in the optical axis direction [31]). The time of flight of the projectile-like residues through the spectrometer was measured on an event-by-event basis between a micro-channel plate (MCP) [32] located in front of the quadrupole magnet and the PPAC detectors of the focal plane. This configuration allowed an unambiguous identification of the transmitted residues in atomic number (Z), mass (A) and charge (Q). The gas pressure in the ionization chamber was adjusted at 86 mbar to stop all projectile-like residues in the last subsection of the ionization chamber. The identification of zinc isotopes is illustrated in Fig. 1.

The prompt gamma rays emitted in flight by the produced nuclei were detected by the AGATA Demon-

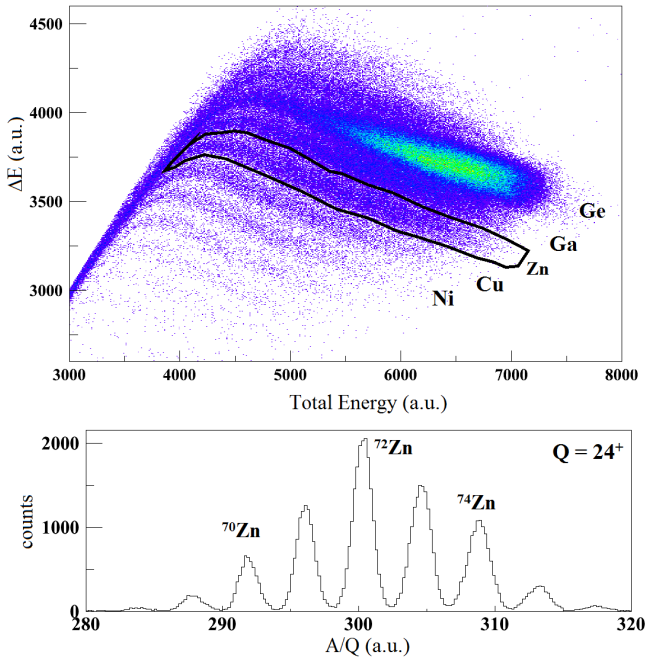

FIG. 1: (color online) Identification of Zn isotopes with PRISMA. *Top:* Energy loss in the two first ionisation chamber subsections versus total energy. *Bottom:* A/Q distribution for Zn isotopes with a selected charge state Q=24^+.

strator, which comprised four triple cluster modules positioned at a distance of 18 cm from the target and covering backward angles between 135° and 175°. With this setup, the simulated full-absorption efficiency is 2.4% for a γ ray of 600 keV. The digitized signal pulses from the 36-fold segmented germanium detectors were compared to a data base of simulated detector responses using a pulse-shape analysis algorithm [33] to determine the loci of the interactions of the γ rays in the germanium crystals. A position resolution of better than 5 mm FWHM was achieved. The energies of individual γ rays were then found by applying a γ-ray tracking algorithm [34]. The entire data processing was performed on-line, even though digitized traces of segment and core events from the AGATA detectors were kept on disk, and energies and positions of the γ rays were stored in list mode together with a time stamp, which allowed correlating the γ rays observed with the AGATA Demonstrator at the target position with the reaction products identified at the focal plane of PRISMA. The digital treatment of the signals allows high counting rates per crystal compared to analogue devices. In the experiment, the average count rate per AGATA crystal was 50 kHz.

Lifetimes were measured using the recoil-distance Doppler shift (RDDS) technique. A Nb foil of 4.2 mg/cm^2 thickness was mounted at a short distance downstream from the target in order to slow the velocity of the reaction products recoiling from the target. The distance between the stretched target and degrader foils was adjusted and controlled by a so-called *plunger* device developed at the University of Cologne [35]. Depending on the lifetime of the excited states, the depopulating γ rays are either emitted before or after reaching the degrader foil. If the flight time between the two foils is of the same order as the lifetime of the excited state, two components are observed for each γ ray corresponding to different velocities and hence different Doppler shifts. The distance between the degrader and the target was controlled with an accuracy of better than 1% by the piezoelectric feed-back system of the plunger device. Data were collected for five distances: 100, 200, 500, 1000 and 1900 μm with an average measuring time of 20 hours per distance. With the choice of distances and the given kinematics of the reaction, the experiment was sensitive to lifetimes between approximately 2 and 50 ps. The introduction of the degrader foil did not significantly deteriorate the mass and Z resolution of the PRISMA spectrometer. The average velocities of the Zn ions before and after passing through the degrader were $\beta = 0.10$ (30(1) μm/ps) and 0.087, respectively. The velocity vector of the ions after passing through the degrader is determined from the reconstruction of their flight path through the PRISMA spectrometer; the velocity before passing through the degrader was calculated from the energy loss in the foil. To produce the γ-ray spectra a Doppler-shift correction was applied using the measured velocity after the degrader. The component corresponding to γ-ray emission after the degrader appears therefore at the correct transition energy, whereas the component corresponding to γ-ray emission before the degrader has a larger Doppler shift and appears at a lower energy when observed under backward angles. In the following the components emitted before and after the degrader will be labelled as fast (index "f") and slow (index "s"), respectively. The choice of degrader material and thickness resulted in a separation of 7 keV between the fast and slow components for a 600 keV transition.

III. DATA ANALYSIS

The validity of our setup and data analysis was tested by reproducing the well-known lifetime of the 2_1^+ state in ^{76}Ge, which was strongly populated by inelastic scattering. The measured lifetime obtained in this experiment is 26.6(6) ps to be compared to the reference value of 25.93(29) ps from the litterature [36]. The separation of the fast and slow components of the $2_1^+ \rightarrow 0_1^+$ transition is illustrated in Fig. 2 for a target-to-degrader distance of 500 μm. The energy resolution is measured to be 3.5 keV FWHM for the slow component at 563 keV. The right part of Fig. 2 shows that a sufficient separation of the components is achieved for all angles covered by the AGATA demonstrator.

The data analysis was focussed on excited states in the

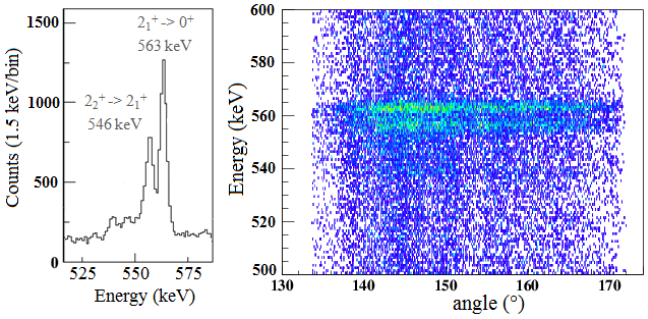

FIG. 2: (color online) *Left:* Part of the Doppler corrected spectrum in coincidence with ^{76}Ge ions identified in PRISMA, showing the $2_1^+ \rightarrow 0_1^+$ transition. The two peaks corresponding to the gamma emitted before and after the degrader are well separated. The two small peaks at lower energy correspond to the $2_2^+ \rightarrow 2_1^+$ transition. *Right:* γ-ray energies plotted as a function of the emission angle with respect to the direction of the recoiling ions.

even-mass isotopes ^{70,72,74}Zn. Mostly states belonging to the yrast band were observed. States up to spin 10^+ have been observed in ^{70}Zn and ^{72}Zn and up to 6^+ in ^{74}Zn. The γ-ray spectra for ^{70,72,74}Zn are presented in Fig. 3 together with partial level schemes.

The even-mass zinc isotopes ^{68,70,72}Zn were previously investigated by Wilson *et al.* in an experiment using deep inelastic scattering between a ^{64}Ni beam and a ^{208}Pb target [37]. In this previous work the yrast cascade of ^{70}Zn was observed up to spin 12^+, and two transitions were reported to feed the 4_1^+ state from non-yrast states: a 1252.1 keV transition from a state assigned as 4^+, and a 1690.1 keV transition from an unassigned state. The former is likely to be the 1251.7 keV transition from a 5^- state that is known from the β-decay of ^{70}Cu [38]. A hint of the 1252 keV transition is visible in our data; it is therefore considered as a feeding transition to extract the lifetime of the 4_1^+ state.

In the case of ^{72}Zn Wilson *et al.* observed the yrast cascade up to spin 10^+ and reported two transitions with energies of 1424.1 and 1526.7 keV, respectively, feeding the 4_1^+ state from non-yrast states [37]. These transitions do not correspond to any of the transitions that were observed to feed the 4_1^+ state after β decay of ^{72}Cu [39]. The spectra taken in the present experiment show some indication for a transition at 1527 keV, decomposed into a fast and slow component. This weak feeding component was taken into consideration for extracting the lifetime of the 4_1^+ state in ^{72}Zn, in addition to the feeding from the 6_1^+ state.

The level scheme of ^{74}Zn was established with tentative spin-parity assignments in β decay studies of ^{74}Cu [40, 41]. Winger *et al.* [40] assigned a spin-parity of 0^+ or 4^+ to the level at 1419 keV since a γ-ray transition of 813 keV was observed to the first excited state at 606 keV, but no direct transition to the ground state. A more detailed study by Van Roosbroeck *et al.* favored a 4^+ assignment for this state [41]. A new transition at 1202 keV was observed and assigned as the $6_1^+ \rightarrow 4_1^+$ transition in ^{74}Zn in an earlier study using the multi-nucleon transfer reaction ^{238}U(^{82}Se,^{74}Zn) [42]. It seems therefore safe to assume that the peaks observed in our experiment in coincidence with ^{74}Zn ions correspond to the yrast sequence up to the 6^+ state as indicated in Fig. 3. Due to the short lifetime of the 6^+ state we only observe the fully shifted component of the $6_1^+ \rightarrow 4_1^+$ transition.

The lifetime analysis was performed using the RDDS method as described by Dewald *et al.* [43]. The lifetime of a given state i is extracted from the intensities I_i^f and I_i^s of the fast and slow components of the transition depopulating the state i. The intensity ratio $Q_i(x) = I_i^s/I_i$ is computed for each distance x, where $I_i = I_i^s + I_i^f$ is the total intensity of the transition. The lifetime for a state i that is fed from higher-lying states k is found for each distance x via

$$\tau_i(x) = -\frac{Q_i(x) - \sum_k \alpha_k Q_k(x)}{v \frac{dQ_i}{dx}(x)}, \qquad (1)$$

where v is the velocity of the ions before reaching the degrader foil. The normalization factors for the feeding transitions $\alpha_k = I_k/I_i$ are independent of the target-to-degrader distance x and were taken as the mean value for all distances. In all three isotopes under study no side feeding into the 2_1^+ state was observed. Their lifetime was consequently extracted from the intensity ratios of the $2_1^+ \rightarrow 0_1^+$ and $4_1^+ \rightarrow 2_1^+$ transitions. As discussed above, side feeding into the 4_1^+ state was observed for ^{70}Zn and ^{72}Zn. Contrary to the $6_1^+ \rightarrow 4_1^+$ transitions, for which the intensity ratios $Q(x)$ could be determined for each distance, this was not possible for the side-feeding transitions due to their weak population. To evaluate their influence on the lifetime of the 4_1^+ states in ^{70}Zn and ^{72}Zn, the intensity ratio was determined from the total spectrum summed over all distances. This integrated intensity ratio allows extracting upper and lower limits for the effective lifetime of the side-feeding state. In case of ^{74}Zn the $6_1^+ \rightarrow 4_1^+$ transition is fully shifted even for the shortest target-to-degrader distances. The effective lifetime of the 6_1^+ state is consequently very short, and the lifetime of the 4_1^+ state can be extracted from the intensity ratios of the $4_1^+ \rightarrow 2_1^+$ transition alone. Errors related to unobserved side feeding into the 4_1^+ state were evaluated in the following way: we estimate that any transition with an intensity of 10% of the $4_1^+ \rightarrow 2_1^+$ transition would be visible in the spectra and take this as an upper limit for unobserved side feeding. We further assume the worst case that the feeding state is long lived with $Q(x) = 1$ for all distances. The influence of such slow unobserved feeding of the 4_1^+ state was used to determine the error of the measured lifetime.

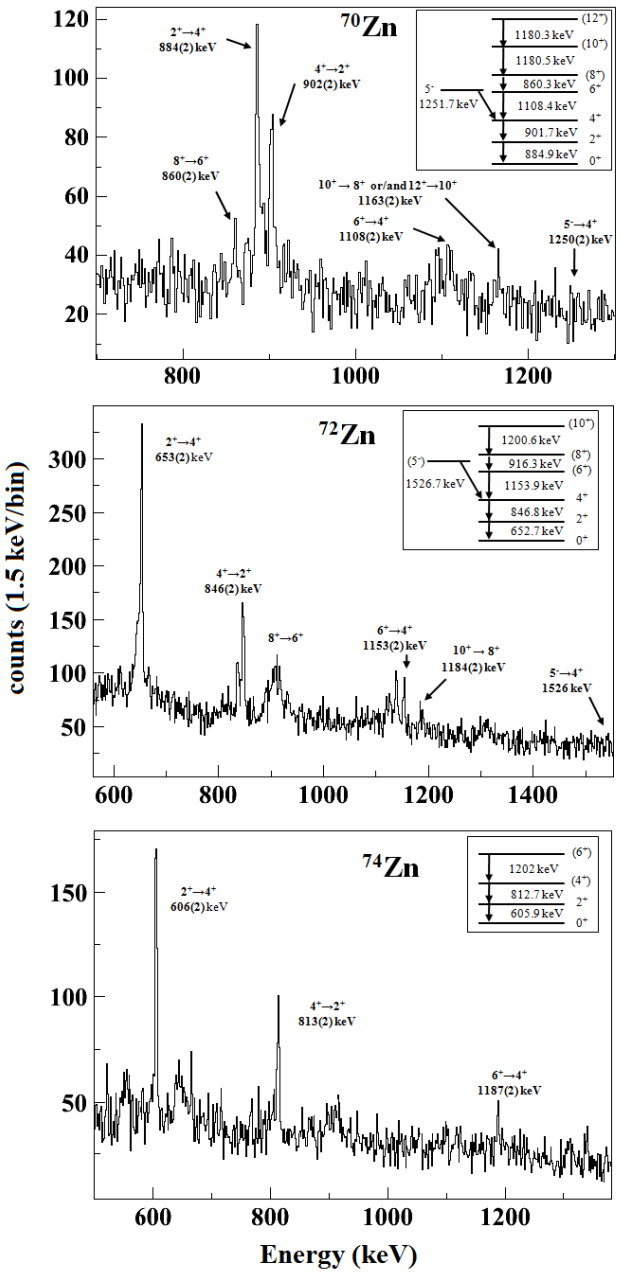

FIG. 3: Gamma-ray spectra in coincidence with ^{70}Zn (top), ^{72}Zn (center), and ^{74}Zn (bottom). The spectra are Doppler corrected on an event-by-event basis for the velocities measured with the PRISMA spectrometer after the degrader foil. The shown spectra were measured with a target-to-degrader distance of 100 μm. Partial decay schemes for the observed transitions are shown in the insets (see text for more details). The broad structures localized at 550 keV, 650 keV and slightly above 900 keV arise from the Doppler correction of the 511 keV line and neutron-induced Ge excitations in the AGATA clusters.

The intensities for the fast and slow components of the transitions were determined by fitting two Gaussians with a constant background to the relevant sections of the γ-ray spectra. The centroids and widths of the Gaussians were allowed to vary within 0.5 and 0.1 keV from their nominal values, respectively, and were then kept constant for all distances. Fig. 4 shows the fits for the $2_1^+ \rightarrow 0_1^+$ and $4_1^+ \rightarrow 2_1^+$ transitions in ^{72}Zn and ^{74}Zn for three target-to-degrader distances of 100, 500 and 1900 μm. The left-hand side of Fig. 5 shows the resulting decay curves, *i.e.* the plot of the ratios $Q(x)$ as a function of the target-to-degrader distance, for the $2_1^+ \rightarrow 0_1^+$ and $4_1^+ \rightarrow 2_1^+$ transitions in ^{74}Zn. The derivative of the decay curves is required for each data point in order to apply the so-called differential decay curve method (*c.f.* eq. 1). The values $dQ_i(x)/dx$ were obtained by fitting two second-order polynomials over separate intervals of the decay curve and taking the derivative of the resulting continuously differentiable function. A data point at distance zero, $Q_i(0) = 1$, was included for all decay curves to improve the quality of the fit. A value for the lifetime of the respective state is obtained for each distance that lies in the region of sensitivity by using equation 1. The right-hand side of Fig. 5 shows the lifetimes obtained for the 2_1^+ and 4_1^+ states in ^{74}Zn at different distances. The final lifetime of a given state is determined as the weighted mean of these values. Deviations from a constant lifetime value over the sensitive range of distances would indicate systematic errors due to the assumed feeding pattern. The consistency of the values obtained for different distances adds confidence to the measurement. It should be noted, however, that the lifetimes measured for the 4_1^+ states in ^{70}Zn and ^{72}Zn are very sensitive to the intensity of the feeding transitions. By not taking into account the side feeding from the 1252 (1527) keV transitions to the 4_1^+ state in $^{70(72)}$Zn, the lifetime of the 4_1^+ state increases by 28 (12) %.

IV. RESULTS AND DISCUSSION

The lifetimes measured for low-lying excited states in ^{70}Zn, ^{72}Zn, and ^{74}Zn are given in Table I. The quoted errors reflect the statistical uncertainty for the intensities of the fast and slow components of the transitions, the uncertainty of the normalization factors for the intensity of the feeding transitions, and the uncertainty in the fit of the decay curve. The highest precision is reached for ^{72}Zn, whereas the errors are larger for ^{70}Zn and ^{74}Zn due to the weaker population of these isotopes. The $B(E2)$ values extracted from the lifetimes are compared to previously published values and to theoretical calculations in Table I and Fig. 6 and will be discussed in the following.

The systematics of $B(E2; 2_1^+ \rightarrow 0_1^+)$ values for the chain of Zn isotopes has been studied and extended in several previous experiments. The $B(E2; 2_1^+ \rightarrow 0_1^+)$

	Experiment					Theory					
			This work		Previous works	SM JUN45		SM LNPS		5DCH Gogny D1S	
	J^π	E (keV)	τ (ps)	B(E2;↓) (e^2fm^4)	B(E2;↓) (e^2fm^4)	E (keV)	B(E2;↓) (e^2fm^4)	E (keV)	B(E2;↓) (e^2fm^4)	E (keV)	B(E2;↓) (e^2fm^4)
^{76}Ge	2^+	563	26.6 (6)	546^{+12}_{-11}	556 (6) [36]	750	562	503	501	770	561
^{70}Zn	2^+	885	5.3 (17)	286^{+131}_{-68}	305 (15) [44]	1116	306	823	327	893	457
					283 (17) [45]						
	4^+	1787	$2.9^{+1.3}_{-1.6}$	475^{+584}_{-147}	720 (70) [46]	2311	401	1557	345	1982	861
^{72}Zn	2^+	653	17.6 (14)	392^{+34}_{-29}	348 (42) [47]	1014	340	636	376	977	392
	4^+	1500	$5.2^{+0.8}_{-0.7}$	361^{+57}_{-47}	–	1982	358	1390	471	2132	768
	6^+	2653	3.0 (9)	134^{+57}_{-31}	–	3119	240	2351	437	3511	1111
^{74}Zn	2^+	606	28.5 (36)	352^{+50}_{-39}	405 (30) [44]	969	339	574	361	964	368
	4^+	1419	$20.0^{+1.8}_{-5.2}$	116^{+32}_{-10}	507 (74) [22]	1740	336	1390	496	2130	724

TABLE I: Experimental lifetimes and B(E2;↓) values for states in ^{76}Ge, ^{70}Zn, ^{72}Zn, and ^{74}Zn and comparison with previously published values, with shell model calculations using the JUN45 effective interaction ($e_p = 1.5e$ and $e_n = 1.1$) [48] and the LNPS interaction ($e_p = 1.4e$ and $e_n = 0.4$) [17], and with calculations using a five-dimensional collective Hamiltonian based on the Gogny D1S interaction [49].

value for ^{74}Zn was measured using three different techniques: a relativistic Coulomb excitation experiment found $B(E2; 2_1^+ \rightarrow 0_1^+) = 408(30) e^2fm^4$ [14], a low-energy Coulomb excitation experiment found 401(32) e^2fm^4 [22], and a Doppler-shift lifetime measurement using a fast fragmentation beam found 370(33) e^2fm^4 [23]. These values are in agreement with our value of 352^{+50}_{-39} e^2fm^4. The systematics of $B(E2; 2_1^+ \rightarrow 0_1^+)$ values indicates a maximum of collectivity at $N \approx 42$, as in the chain of Ge and Se isotopes.

The Coulomb excitation probability measured by Van de Walle *et al.* [22] for the 2_1^+ state in ^{74}Zn depends both on the transitional matrix element $< 0_1^+ || \mathcal{M}(E2) || 2_1^+ >$ and on the diagonal matrix element $< 2_1^+ || \mathcal{M}(E2) || 2_1^+ >$. The $B(E2)$ value quoted above for the low-energy Coulomb excitation experiment was derived under the assumption that $< 2_1^+ || \mathcal{M}(E2) || 2_1^+ > \; = 0$. Since the lifetime of the 2_1^+ state depends only on the transitional matrix element, it is possible to combine the two measurements in order to obtain information on the diagonal matrix element, which is directly related to the nuclear shape. When combined with the data shown in Fig. 9 of Ref. [22], the lifetime measured in the present experiment favors an oblate shape for ^{74}Zn in its 2_1^+ state.

The results obtained in the present experiment for the 4_1^+ states in the three Zn isotopes under study deserve special attention. The systematics of the $B(E2; 4_1^+ \rightarrow 2_1^+)$ values for the chain of Zn isotopes are shown in the lower part of Fig. 6. Our result for $B(E2; 4_1^+ \rightarrow 2_1^+)$ in ^{70}Zn has very large error bars due to the low statistics and to the uncertainty related to its feeding. Because of the large uncertainties, our measurement is unable to shed more light on the surprisingly large $B(E2; 4_1^+ \rightarrow 2_1^+)$ value measured by Mucher *et al.* [46] using the Doppler shift attenuation method.Further lifetime or Coulomb excitation measurements are required in order to determine the collectivity of the 4_1^+ state and resolve other discrepancies, *e.g.* for the 2_2^+ state [46].

The lifetime of the 4_1^+ state in ^{72}Zn was measured for the first time in the present experiment. The resulting $B(E2)$ value is larger than those of the lighter Zn isotopes with $N < 40$, which is expected and can partly be attributed to the role of the $\nu g g_{9/2}$ orbital.

The $B(E2; 4_1^+ \rightarrow 2_1^+)$ value measured for ^{74}Zn, on the other hand, is very small. It is much smaller than the one measured for ^{72}Zn,and there is a significant discrepancy between the $B(E2)$ value from our lifetime measurement and the low-energy Coulomb excitation experiment of Van de Walle *et al.* [22].

In order to understand this surprising result and the discrepancy with the Coulomb excitation measurement, we have thoroughly investigated experimental biases that could lead to a longer lifetime for the 4_1^+ state in ^{74}Zn. The possibility of a long-lived state feeding the 4_1^+ state was considered in particular. If such a state existed, it would appear to influence only the measured lifetime of the 4_1^+ state, but not that of the 2_1^+ state, which is in very good agreement with all previous measurements. The non-observation of a slow feeding transition in the γ-ray spectra could then only be explained by two possible scenarios: *i)* The state lies just above the 4_1^+ state, resulting in a very low transition energy which lies below the threshold of the

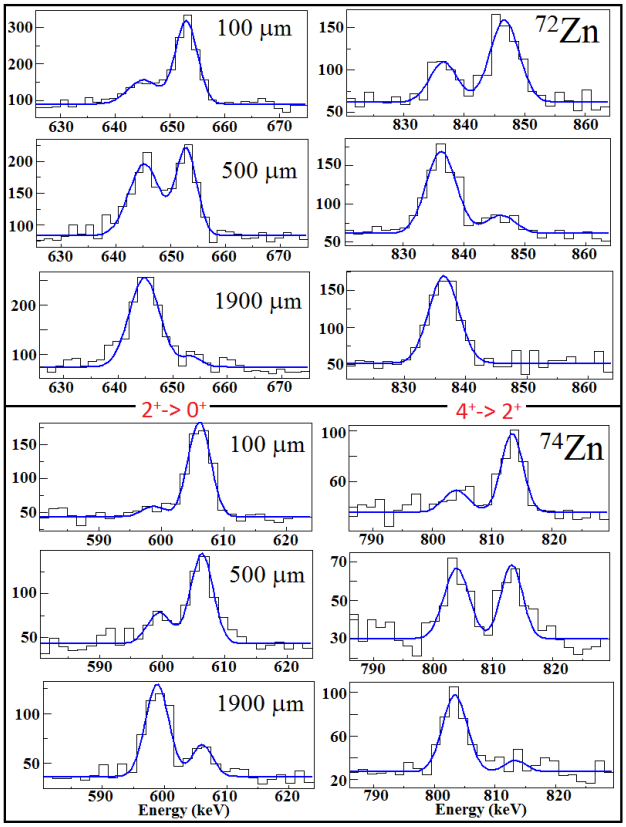

FIG. 4: (color online) Partial spectra for ^{72}Zn (upper part) and ^{74}Zn (lower part) showing the $2_1^+ \rightarrow 0_1^+$ (left) and $4_1^+ \rightarrow 2_1^+$ transitions (right) for three different target-to-degrader distances as indicated. The measured spectra are shown as histograms and the Gaussian fits as full (blue) lines. The evolution of the fast and slow components as a function of distance is clearly visible.

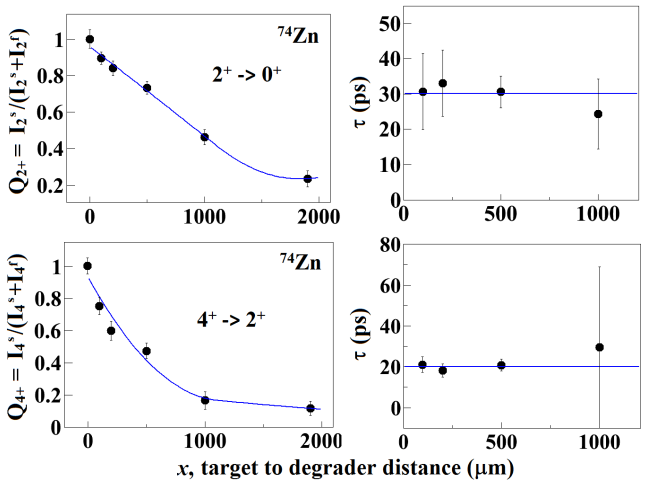

FIG. 5: Decay curves for the $2_1^+ \rightarrow 0_1^+$ and $4_1^+ \rightarrow 2_1^+$ transitions in ^{74}Zn (left). The data points were fitted by a continously differentiable function of piecewise defined second-order polynomials (splines). The right-hand side of the figure shows the resulting lifetimes obtained for different target-to-degrader distances. The horizontal line indicates the weighted mean value.

AGATA detectors of approximately 50 keV. Such a state would furthermore have to have $I \geq 5$; otherwise its decay to the 2_1^+ or 0_1^+ state should be seen. There is, however, no evidence for such a state, neither from other experiments investigating ^{74}Zn, nor in neighboring nuclides of this mass region, and we consider such a scenario as highly unlikely. *ii)* The feeding state is only weakly populated, so the transition cannot be separated from the background, but it has a very long lifetime. As discussed earlier, this possibility was included in the error analysis and can hence not explain the long lifetime measured for the 4_1^+ state in ^{74}Zn.
Due to the detection in the PRISMA spectrometer, it is possible to measure the excitation energy of the reaction product on an event-by-event basis, albeit only with limited resolution. In this way it is possible to select events in which the multi-nucleon transfer reaction directly populates states at low excitation energy, and to exclude events where the same states are fed via γ decay from higher-lying states, thereby eliminating the influence of feeding transitions on the lifetime measurement for a low-lying state [50, 51]. We have applied this technique in the case of ^{72}Zn, where the relatively high level of statistics allows applying such conditions. The suppression of events corresponding to high excitation energies in ^{72}Zn had no influence on the lifetime extracted for the 4_1^+ state, which suggests that the feeding from higher-lying states is well under control. Unfortunately it was not possible to perform the same analysis for ^{74}Zn due to the lower level of statistics.

We now compare the transition probabilities obtained for ^{70,72,74}Zn with beyond-mean-field calculations using the Gogny D1S interaction [52, 53] in a 5-dimensional Collective Hamiltonian (5DCH) formalism that takes into account quadrupole degrees of freedom [49]. This approach has already given satisfactory results regarding the question of the collectivity of N = 40 nuclei [54]. The 5DCH approach consistently overestimates the transition probabilities in the zinc isotopes from N=32 to N=50. B(E2;$2_1^+ \rightarrow 0_1^+$) are calculated approximately 30% above the experimental value whereas the B(E2;$4_1^+ \rightarrow 2_1^+$) values are overestimated by a factor of 2 to 3. The vicinity of zinc isotopes to the Z=28 shell closure may indicate that the collective degrees of freedom considered in this approach are not sufficient to correctly describe their spectroscopy. In Fig. 7, one can see that excitation energies of the first 4^+ and 2^+ states for N>40 are overestimated in the present 5DCH approach.

We further compare our results to shell-model calculations using the JUN45 interaction which was developed to reproduce correctly the spectroscopy of nuclei in the $pf_{5/2}g_{9/2}$ valence space with a ^{56}Ni core [48]

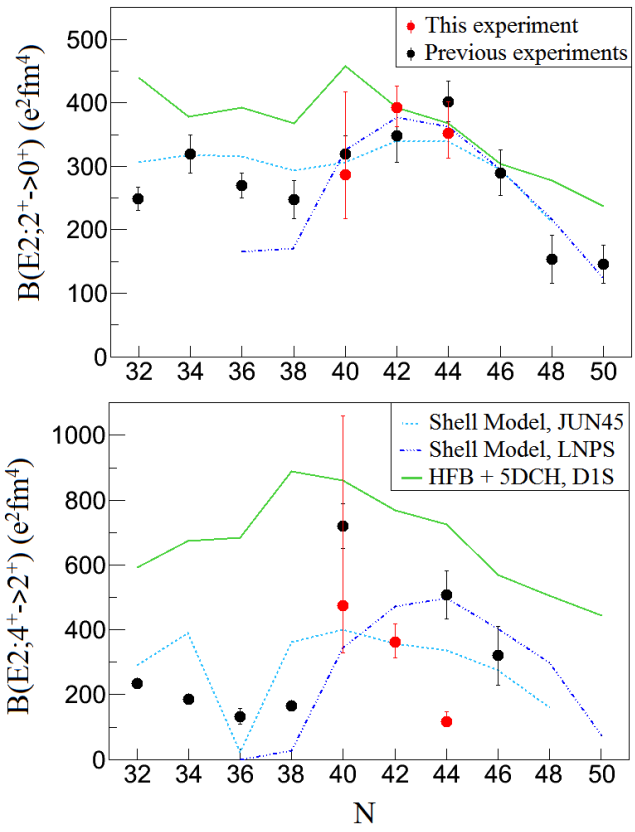

FIG. 6: (color online) Results from the present experiment and systematics of experimental $B(E2;2_1^+ \rightarrow 0_1^+)$ and $B(E2;4_1^+ \rightarrow 2_1^+)$ values for the chain of Zn isotopes. Theoretical values were calculated with the shell model using the JUN45 interaction in the $pf_{5/2}g_{9/2}$ valence space (^{56}Ni core, $e_p = 1.5e$ and $e_n = 1.1$) [48], the LNPS interaction in the $pfg_{9/2}d_{5/2}$ valence space (^{48}Ca core, $e_p = 1.4e$ and $e_n = 0.4$) [17] and with a five-dimensional collective Hamiltonian using the Gogny D1S force [49].

and the LNPS interaction developed for the extended $pf_{5/2}g_{9/2}d_{5/2}$ valence space with a ^{48}Ca core [17]. In this latter case, calculations have been performed allowing up to 10 particles to be excited across N=40 and Z=28. It is worth reminding that the extension to a larger valence space than $pf_{5/2}g_{9/2}$ has indeed been shown to be crucial to reproduce the spectroscopy of N∼40 neutron-rich nuclei in the region of heavy Fe and Cr isotopes [15, 16, 19], in particular a ^{56}Ni core has been claimed to be inappropriate in some cases [55]. In the following, predictions are given for non standard effective charges: ($e_p = 1.5e$ and $e_n = 1.1$) are used for JUN45 since they allow a better agreement with data on which the predictions have been tested in the orginal paper [48], ($e_p = 1.4e$ and $e_n = 0.4$) are used for LNPS, as they allow a better agreement with spectroscopic information in Cr isotopes [19].
Comparisons of the data with the two shell model predictions show a fair agreement for the B(E2;$2_1^+ \rightarrow 0_1^+$) and B(E2;$4_1^+ \rightarrow 2_1^+$) systematics. However, even though shell model predictions for the transition probabilities B(E2;$4_1^+ \rightarrow 2_1^+$) with the JUN45 and LNPS interactions are in agreement for the ^{70,72}Zn isotopes, they do not reproduce the strong reduction observed in this work from ^{72}Zn to ^{74}Zn. Very small $B(E2;4_1^+ \rightarrow 2_1^+)$ values are found experimentally for $^{62-66}$Zn. Almost vanishing values are indeed predicted in the case of ^{66}Zn within the shell model formalism. In ^{66}Zn, the two protons above the Z=28 gap are predicted to have a large component on the $p_{3/2}$ orbital in the ground state and cannot be coupled to spin 4^+ whereas, at N=40, an orbital inversion occurs between the $\pi p_{3/2}$ and the $\pi f_{5/2}$ orbitals, and the two valence protons, with a large component on the $f_{5/2}$ orbital, can easily coupled to 4^+. From the shell model description, we threfore do not expect such an hindrance of $B(E2;4_1^+ \rightarrow 2_1^+)$ to occur in heavier ^{72,74}Zn [56].
Note that, as shown in Fig. 7, the shell model using a $pf_{5/2}g_{9/2}$ valence space and a ^{56}Ni core overestimates the excitation energies of the first excited 2_1^+ and 4_1^+ states from N = 40, while the shell model predictions using the LNPS interaction and an extended valence space reproduce very well the first 2^+ and 4^+ excitation energy over the whole systematics.

Today, no firm conclusion can be raised to understand the discrepancies beetween the predicted B(E2;$4_1^+ \rightarrow 2_1^+$) systematics and the experimental one from this work, especially the fast drop occuring between ^{72}Zn and ^{74}Zn. If the present experimental result is confirmed, one can already exclude potential origins of such a low B(E2;$4_1^+ \rightarrow 2_1^+$) value for ^{74}Zn from the comparison of the different model predictions: (i) could an explicit tensor term in the effective NN interaction, missing in the Gogny force, allow to better reproduce the structure properties of zinc isotopes including the $B(E2;4_1^+ \rightarrow 2_1^+)$ and the value of the 4_1^+ excitation energies? The present shell model calculations naturally include such a tensor term with no prediction of very low B(E2;$4_1^+ \rightarrow 2_1^+$) in ^{74}Zn. (ii) Does the valence space be responsible of such discrepancies? The inclusion of the $d_{5/2}$ orbital in the shell model valence space and the extension to a ^{48}Ca core lead to a better agreement with the excitation energy data but it also leads to larger transition probabilities than those calculated with JUN45, with no help to further understand the drop of B(E2;$4_1^+ \rightarrow 2_1^+$) from ^{72}Zn to ^{74}Zn, as shown in Fig. 6. This might indicate that the observed low B(E2;$4_1^+ \rightarrow 2_1^+$) in ^{74}Zn is not the consequence of a too small valence space.
It is interesting to note that shell model calculations with the LNPS interaction predict prolate deformation for both 2^+ and 4^+ states in the three Zn isotopes, but these states do not belong to a rotational band. Along the isotopic chain, it is observed that for the first excited states the occupation of neutrons in the $g_{9/2}$ and $d_{5/2}$ increases abruptly when passing from N=38 to N=40.

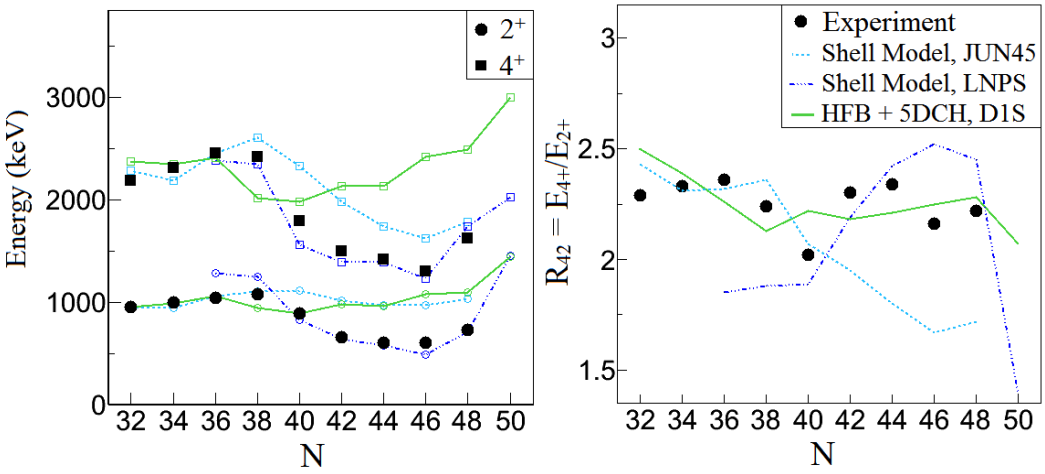

FIG. 7: (color online) The left panel shows experimental excitation energies of the 2^+ (dot symbols) and 4^+ states (square symbols) for the chain of Zn isotopes and a comparison with theoretical calculations. The right panel shows the ratio $R_{42} = E(4_1^+)/E/2_1^+$). The theoretical calculations are based on the shell model (dotted and dashed blue lines) with the JUN45 [48] and LNPS [17] interactions (see text for details) and on a five-dimensional collective hamiltonian (green line) used with the Gogny D1S force [49].

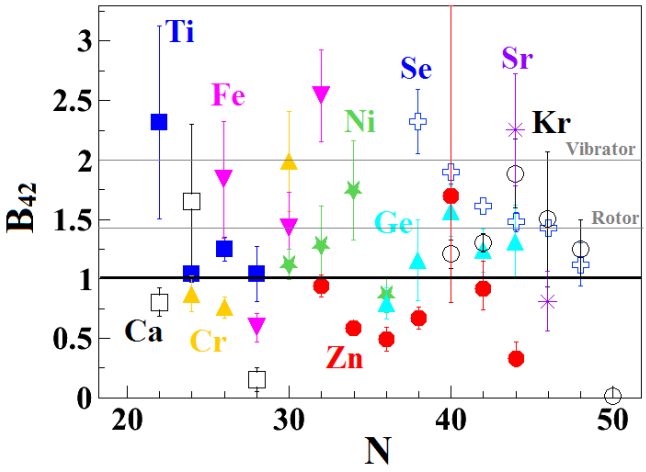

FIG. 8: (color online) Ratio of experimental B(E2;$4_1^+ \rightarrow 2_1^+$)/B(E2;$2_1^+ \rightarrow 0_1^+$) for nuclei with Z = 20 to Z = 40. Zinc isotopes are represented by red dots.

For collective excitations, the ratio B_{42}=B(E2;$4_1^+ \rightarrow 2_1^+$)/B(E2;$2_1^+ \rightarrow 0_1^+$) is expected to be larger than 1: in the harmonic oscillator model it is equal to 2, whereas in the rotor model it is equal to 1.43. A systematics of this ratio for medium mass nuclei with N from 20 to 50 is shown in Fig. 8. This plot can be seen as complementary to the one for heavier nuclei published in [24]. Among the available data in this mass region, the zinc isotopes have the lowest B_{42} ratio, signing non collective excitations. This observation is consistent with their vicinity to the closed shell nickel isotopes. As stated in [24, 57], the only situation where a B_{42} ratio lower than one occurs is when the seniority is a good quantum number. In such situation, the B(E2;$2_1^+ \rightarrow 0_1^+$) increases up to mid shell whereas the B(E2;$4_1^+ \rightarrow 2_1^+$) decreases. The B_{42} systematics for zinc isotopes seems to indicate such a behavior with a maximum at N=40 and a lowering of B_{42} towards N=44. The experimental measurement of such a ratio for heavier zinc isotopes and nickel isotopes from ^{68}Ni toward ^{78}Ni would be of interest to tackle this question.

Finally, the B(E2) systematics for ^{72}Zn from the $2_1^+ \rightarrow 0_1^+$ to the $6_1^+ \rightarrow 4_1^+$ transition drops for $6_1^+ \rightarrow 4_1^+$. This trend is predicted by shell-model calculations with the JUN45 interaction in fairly good agreement with our measurement, but fail to describe the excitation energy of the 6^+ state. On the other hand, calculations with the LNPS interaction reproduce quite well the energy of the states and predicts a decrease of the B(E2) value, but much slower that the data. The 5DCH approach does not describe this behavior but instead a steep increase of the B(E2) values with increasing spin, another indirect indication that long-range correlations may not be sufficient to describe the low-lying structure of this neutron-rich zinc nuclei.

V. SUMMARY

In summary, lifetimes of low-lying states in ^{70,72,74}Zn have been measured using the RDDS technique and the AGATA demonstrator coupled to the PRISMA magnetic spectrometer. Regarding the first 2_1^+ state, a maximum of collectivity is found at N = 42, as in the case of Ge and Se isotopic chains. The measured lifetimes of the first 2_1^+ states in ^{70,72,74}Zn from this experiment are in very good agreement with previous measurements. In the case of the first 4_1^+ states, the

values obtained in the present work contradict previous measurements from which smaller lifetimes were systematically deduced. A strong drop in B(E2;$4_1^+ \rightarrow 2_1^+$) systematics is observed at N = 44, but not reproduced so far neither by shell model nor mean field approaches. The present experimental study suggests that the nature of the low-lying excitation in neutron-rich zinc isotopes is similar to those of stable zinc isotopes with a ratio B(E2;$4_1^+ \rightarrow 2^+$)/B(E2;$2_1^+ \rightarrow 0_1^+$) lower than one. Neither shell model predictions with the JUN45 or LNPS interaction nor collective hamiltonian calculations with the Gogny force reproduce this feature. In addition, the B(E2;$6_1^+ \rightarrow 4_1^+$) has been measured to be 134^{+57}_{-31} e^2fm^4 in ^{72}Zn much lower than the B(E2) values corresponding to the decay of the 4_1^+ and 2_1^+ states. This tendency is qualitatively reproduced by shell model predictions.
The effect of side feeding has been carefully taken into account in the present work. The present study illustrates that lifetime measurements with the RDDS technique using deep inelastic scattering that populates high-excitation-energy states requires sufficient statistics to quantify weak side feeding from off-band states that have a significant impact on the lifetime extraction. Saying so, we conclude that lifetimes in neutron-rich zinc isotopes deserve additional investigations on both experimental and theoretical sides. In particular, the confirmation of the unexpectedly long lifetime of the 4_1^+ state of ^{74}Zn and the extension of the systematics to richer neutron-rich even-even zinc isotopes are called for.

The authors would like to thank F. Nowacki and K. Sieja for enlightening discussions and their suggestions to improve the manuscript. The authors are grateful to the ALPI accelerator team for quality of the beam delivered during the experiment. B. Lommel and J. Steiner from the GSI are acknowledged for their help in preparing the Uranium target and the opportunity to use the GSI target laboratory.

[1] M.G. Mayer, Phys. Rev. **74**, 235 (1948).
[2] M.G. Mayer, Phys. Rev. **75**, 1969 (1949).
[3] O. Haxel, J.H.D. Jensen, H.E. Suess, Phys. Rev. **75** 1766, (1949).
[4] C. Détraz *et al.*, Phys. Rev. C **19**, 164 (1979).
[5] T. Motobayashi et al., Phys. Lett. **B 346**, 9 (1995).
[6] A. Obertelli *et al.*, Phys. Lett. **B633**, 33 (2006).
[7] R. Kanungo *et al.*, Phys. Rev. Lett. **102**, 152501 (2009).
[8] T. Otsuka *et al.*, Phys. Rev. Lett. **87**, 082502 (2001).
[9] T. Otsuka *et al.*, Phys. Rev. Lett. **95**, 232502 (2005).
[10] T. Otsuka *et al.*, Phys. Rev. Lett. **105**, 032501 (2010).
[11] J.D. Holt *et al.*, arXiv:1009.5984v2 (2011).
[12] S. Franchoo *et al.*, Phys. Rev. C **64**, 054308 (2001).
[13] K. T. Flanagan *et al.*, Phys. Rev. Lett. **103**, 142501 (2009).
[14] O. Perru *et al.*, Phys. Rev. Lett. **96**, 232501 (2006).
[15] J. Ljungvall *et al.*, Phys. Rev. C **81**, 061301 (2010).
[16] W. Rother *et al.*, Phys. Rev. Lett. **106**, 022502 (2011).
[17] S. M. Lenzi, F. Nowacki, A. Poves, K. Sieja, Phys. Rev. C **82**, 054301 (2010).
[18] N. Aoi *et al.*, Phys. Rev. Lett. **102**, 012502 (2009).
[19] T. Baugher *et al.*, Phys. Rev. C **86**, 011305 (2012).
[20] S. Naimi *et al.*, Phys. Rev. C **86**, 014325 (2012).
[21] J.M. Daugas *et al.*, Phys. Rev. C **83**, 054312 (2011).
[22] J. Van de Walle *et al.*, Phys. Rev. C **79**, 014309 (2009).
[23] M. Niikura *et al.*, Phys. Rev. C **85**, 054321 (2012).
[24] R. B. Cakirli *et al.*, Phys. Rev. C **70**, 047302 (2004).
[25] E. Williams *et al.*, Phys. Rev. C **74**, 024302 (2006).
[26] D. Radeck *et al.*, Phys. Rev. C **85**, 014301 (2012).
[27] S. Akkoyun *et al.*, Nucl. Instr. Meth. A **668**, 26 (2011).
[28] A. Gadea *et al.*, Nucl. Instr. Meth. A **654** (2011) 88-96.
[29] A.M. Stefanini *et al.*, Nucl. Phys. A **701**, 217c (2002).
[30] S. Beghini *et al.*, Nucl. Instr. Meth. A **551** (2005) 364-374.
[31] S. Szilnet *et al.*, Phys. Rev. C **76**, 024604 (2007).
[32] G. Montagnoli *et al.*, Nucl. Instr. Meth. A **547** (2005) 455-463.
[33] R. Venturelli and D. Bazzacco, LNL Annual report 2004, INFN-LNL, Legnaro, Italy (2005) 220.
[34] A. Lopez-Martens *et al.*, Nucl. Instr. Meth. A **533** (2004) 454-466.
[35] A. Dewald, in Ancillary Detectors and Devices for Euroball, edited by H. Grawe (GSI and the Euroball Ancillary Group, Darmstadt, 1998), p. 70.
[36] R. Lecomte *et al.*, Phys. Rev. C **22**, 1530 (1980).
[37] A.N. Wilson *et al.*, Eur. Phys. J A **9**, 183 (2000).
[38] J. Van Roosbroeck *et al.*, Phys. Rev. C **69**, 034313 (2004).
[39] J.-C. Thomas *et al.*, Phys. Rev. C **74**, 054309 (2006).
[40] J.-A. Winger *et al.*, Phys. Rev. C **39**, 1976 (1989).
[41] J. Van Roosbroeck *et al.*, Phys. Rev. C **71**, 054307 (2005).
[42] T. Faul, PhD thesis, University of Strasbourg (2007).
[43] A. Dewald, S. Harissopulos, and P. von Brentano, Z. Phys. A **334**, 163 (1989).
[44] B. Pritychenko *et al.*, At. Data and Nucl. Data Tables **98**, 798 (2012).
[45] J. K. Tuli, Nuclear Data Sheets **103**, 389 (2004).
[46] D. Mücher *et al.*, Phys. Rev. C **79**, 054310 (2009).
[47] S. Leenhardt *et al.*, Eur. Phys. J. A **14**, 1-5 (2002).
[48] M. Honma *et al.*, Phys. Rev. C **80**, 064323 (2009).
[49] J.-P. Delaroche *et al.*, Phys. Rev. C **81**, 014303 (2010).
[50] D. Mengoni *et al.*, Eur. Phys. J. A **42**, 387-391 (2009).
[51] A. Dijon *et al.*, Phys. Rev. C **83**, 064321 (2011)
[52] J. Dechargé, and D. Gogny, Phys. Rev. C **21**, 1568 (1980).
[53] J.-F. Berger, M. Girod, and D. Gogny, Comput. Phys. Commun. **63**, 365 (1991).
[54] L. Gaudefroy *et al.*, Phys. Rev. C **80**, 064313 (2009).
[55] K. Sieja and F. Nowacki, Phys. Rev. C **81**, 061303(R) (2010).
[56] F. Nowacki, private communication (2012).
[57] J. J. Ressler *et al.*, Phys. Rev. C **69**, 034317 (2004).